Reaction Kinetics, Mechanisms and Catalysis (2023) 136:2617–2638
https://doi.org/10.1007/s11144-023-02478-w

Kinetic modeling of bio-based heterogeneously catalyzed lard oil methanolysis in methyl ester production

C. B. Ezekannagha[1] · O. D. Onukwuli[2] · C. F. Uzoh[2] · C. N. Eze[3]

Received: 13 July 2023 / Accepted: 13 August 2023 / Published online: 23 August 2023

Abstract

The kinetic modeling of bio-based heterogeneously catalyzed lard oil methanolysis in lard oil methyl ester (LOME) synthesis was investigated. To describe the reaction, the reverse basic reaction mechanism of transesterification was employed. The transesterification reaction was performed within a time range of 0–3.5 h at varying temperatures of 50 °C, 55 °C and 60 °C and optimum reaction conditions of methanol to oil molar ratio 10.5:1, 2.5 wt% catalyst quantities. The variations in concentration of the reactants and LOME against time and temperature reveal substantial changes from 0 to 1.5 h beyond which the reactant consumption and product formation remained constant across the defined temperature readings. The reaction was observed to be favored at high temperature. The rate equation based on the assumption of triglycerol to diglycerol conversion as rate limiting in the reverse basic reaction mechanism was observed to be the best satisfactory representation of the experimental data. The activation energy and frequency factor were determined as 20.54 kJ/mol and 1960 h^{-1}. The extrapolative competency of the obtained model was verified with experimental data which exhibited satisfactory correlation.

Keywords Calcined banana peel ash catalyst (CBPA) · Kinetics · Lard oil · Modeling · Reverse basic mechanism

✉ C. B. Ezekannagha
contactchy20@gmail.com

[1] Department of Chemical Engineering, Madonna University, Akpugo Campus, Enugu State, Nigeria

[2] Department of Chemical Engineering, Nnamdi Azikiwe University P.M.B. 5025, Awka, Anambra State, Nigeria

[3] Department of Chemical Engineering, Chukwuemeka Odumegwu Ojukwu University, Uli, Anambra State, Nigeria

Introduction

The dependence of the global economy on energy is excessive and is likely to intensify due to the exponential increase in population and the hunt for good life. The conventional energy source (natural gas, coal and oil) used as source of energy supply poses some inherent risk in its use [1]. This risk is associated with the fossil fuel depletion with no immediate replacement and greenhouse gas effect emanating from burning of the conventional fuel. These challenges necessitated the search for a renewable, environmentally friendly and cost effective alternative fuel. An alternative fuel to replace the fossil fuel must be renewable, environmentally friendly, readily available, technically feasible and economically acceptable [2, 3]. A viable alternative fuel is methyl ester. Methyl ester is a renewable fuel that is composed of mono alkyl esters of long chain fatty acids synthesized by the transesterification reaction of oil or fat using an alcohol in the existence of a catalyst [4, 5]. A key limitation in the wide spread methyl ester synthesis is the production cost arising mainly from the cost of the feedstock and as such effort should be geared towards the reduction of the cost of oil and catalyst used as feedstock [6]. Ude and Onukwuli [7] stated that various sources for methyl ester production abound. However, attention should be given to methyl ester production from waste (oil and catalyst) for production cost mitigation so as to enable the derived bio-fuel competes favorably with the conventional diesel fuel. Animal fats, waste vegetable oil and micro algal oil constitute the foremost sustainable feedstock for methyl ester synthesis. The utilization of edible oils for example palm oil, sunflower, soybeans, groundnut oil etc. for methyl ester production will add to the production cost due to its soaring cost in addition to scarcity of the oils for cooking intents [8]. Lard oil is a by-product of the pork rendering process, which can be categorized as an inexpensive feedstock available for methyl ester synthesis. It is also an attractive economic alternative in the case of break out of pork diseases or where parts of the animal have been banned for human consumption due to health condition. On the other hand, banana waste peels are comparatively cost free and the utilization as catalyst in transesterification reaction will simultaneously serve as means of waste disposal and waste upgrade to energy. A plethora of researchers have reported homogeneously catalyzed transesterification of oil in methyl ester synthesis from diverse sources with either sodium hydroxide or potassium hydroxide at laboratory and industrial level [9–12]. The numerous advantages associated with homogeneous catalysis of the transesterification process include process simplicity, high biodiesel yield, faster reaction rate and shorter reaction time with associated drawbacks such as equipment corrosion, non-easy to separate, non-renewability and recyclability and downstream waste treatment [13, 14]. The water washing and purification stages required to achieve the fuel quality standard lead to increase in the production cost [15]. Quite the reverse, the use of heterogeneous catalysts for methyl ester synthesis appears to be more effectual and viable due to the following; ease in separation, recyclability, non-corrosive and environmental benign characteristics [16]. Subsequently, the substitution of homogeneous catalyst with heterogeneous catalyst has been acceptable currently.

Few researchers have reported transesterification process with calcined banana peel ash (CBPA) as catalyst [17, 18]. Excellent catalytic ability was exhibited as methyl ester yield above 95% was recorded by the researchers. The studies were mainly based on how to synthesize the catalyst, characterization and the catalytic activity. There is paucity of literature on the function of most of these bio-based derived catalysts. Other important variables that need to be given attention in the functionality of the catalysts in a transesterification reaction are the reaction mechanism and the rate limiting step [19]. Hence the model will be based on the reverse basic mechanism (RB) of transesterification reaction proposed by Freedman. A kinetic model is required to figure out how the synthesized catalyst functions and its application furthermore at industrial level. The reaction kinetics becomes pertinent in the estimation of the degree of the reactants change and product formation at all times within specified terms. The information is similarly required by process/chemical engineers in designing and optimizing reactor systems for a specified catalyzed transesterification reaction [20]. Methanol adsorption has been reported as the rate controlling step in some of the heterogeneously catalyzed transesterification reaction of oil with methanol while in other scenarios, the surface reaction between triglyceride and methanol have been ascertained as the slowest step or the rate limiting step in the transesterification process [19, 21]. Consequently, this research centers on developing a kinetic model which describes the transesterification of lard oil in lard oil methyl ester production by expending calcined banana peel ash (CBPA) catalyst.

Materials and methods

Materials

Ripe banana peels were obtained from home-based waste, waste pork lard used for lard oil synthesis in the transesterification reaction was obtained from New market Enugu, methanol (CH_3OH, 99.8% purity) and other chemicals/reagents were purchased from Conraws company ltd. Enugu. All the chemicals and reagents used were of analytical grade.

Methods

Lard oil synthesis and characterization

The pork fat was extracted using dry-rendering method by exposing it to heating in a pan in the absence of water at 110 °C for 1 h (at atmospheric pressure to circumvent any degradation) to eliminate water, waxy, as well as suspended and residual matters. The rendering method is in accordance to the approach used by Alptekin et al. [22] and Ezekannagha et al. [10]. Liquefied fat was subsequently purified to eliminate the non-soluble constituents known as cracklings. The physico-chemical parameters of the synthesized lard oil were determined according to the American

Standard for Testing and Materials (ASTM) method was conducted. The processed lard oil was kept in an air tight opaque plastic jar to inhibit oxidation.

Catalyst synthesis from ripe banana peels

The discarded banana peels from ripe banana fruits were removed manually. The collected waste peels were reduce to small pieces to accelerate the drying process. The small sized waste peels were thoroughly washed with distilled water thrice to remove impurities after which they were sun-dried. The dried banana peels were then burnt completely in open air to produce ash and further grounded to ash catalyst powder with a mixed blender. The burnt powdered banana ash catalyst was thermally treated via calcination in a muffle furnace at a temperature of 700 °C for 4 h for activation and to obtain calcined banana peel ash CBPA [17, 23]. Finally, it was put away in an air tight vessel for extended use as heterogeneous base catalyst in the synthesis of the lard oil methyl ester.

Ripe banana peel ash catalyst characterization

The synthesized bio-based heterogeneous base catalysts, uncalcined banana peel ash UBPA and calcined banana peel ash, CBPA were characterized with Energy dispersive atomic x-ray spectroscopy (EDAX) to ascertain the chemical compositions, Fourier Transform Infra-Red (Model: Agilent Cary 630) FTIR Spectrometer to detect the functional groups in the wavelength range of 4000–650 cm^{-1}, X-ray diffraction (XRD) using Rigaku miniflex-600 diffractometer (Cu-Kα radiation, $\lambda = 1.5406$ Å) in 2Θ range 2°–70° for the major component phase/group present. Scanning electron microscope (SEM) was used to determine the morphology structure while Brunauer–Emmett–Teller (BET) analysis conducted using Quantachrome NovaWin Nova 4200E was used to measure the surface area, pore volume and pore size of the catalyst sample.

Transesterification reaction

50 g of lard oil was added into a 250 ml three-necked round bottom batch reactor fitted with a reflux condenser, temperature indicator placed on a heating mantle with magnetic stirrer. The oil was preheated to remove any trace water present. Preceding the use of the catalyst, 2.5 wt% CBPA catalyst (based on the oil weight) was partly dissolved in 14 ml (10.5:1) of methanol. The mixture was then added slowly to the heated oil in the batch reactor and the temperature maintained at 50 °C with a constant speed of 300 rpm for 3.5 h. 5 ml of the reaction sample was taken out in a beaker and cooled in a water bath to prevent extended reaction from taking place. Samples were withdrawn at 30 min time interval. The transesterification products were then analyzed and characterized as a function of time and temperature employing Gas chromatography—mass spectrometer (GC–MS). The same procedure was repeated for the defined temperature readings at 55 °C and 60 °C. Basic calibration curves for the lard oil methyl ester were made with n-octane taken as an internal benchmark. The percentage areas were changed to mass percentages for all

constituents of the samples by using the standard calibration charts prepared. A plot of concentration of the species, CH_3OH, T, D, M, B and G against time at 50 °C, 55 °C and 60 °C were done. The symbols CH_3OH, T, D, M, B, and G were used to represent the strength of methanol, triglyceride, diglyceride, monoglyceride, biodiesel and glycerol.

Kinetic modeling

Rate equations were derived based on the reverse basic mechanism of transesterification reaction proposed by Freedman in transesterification of triglyceride to model the kinetics of the heterogeneously catalyzed lard oil transesterification. Equation 1 expresses the general equation for transesterification process.

$$TG + 3ROH \overset{CBPA}{\longleftrightarrow} G + 3ME \tag{1}$$

The basic reaction mechanism of transesterification is as shown in Eqs. 2–4. Each step in the sequence of the three steps of transesterification reaction with methanol is seen to consume one mole of methanol to produce one mole of methyl ester (biodiesel).

$$T + CH_3OH \underset{k_2}{\overset{k_1}{\longleftrightarrow}} D + B \tag{2}$$

$$D + CH_3OH \underset{k_4}{\overset{k_3}{\longleftrightarrow}} M + B \tag{3}$$

$$M + CH_3OH \underset{k_6}{\overset{k_5}{\longleftrightarrow}} G + B \tag{4}$$

Here T, CH_3OH, D, B, M, and G correspond to the concentration of triglyceride, methanol, diglyceride, biodiesel, monoglyceride and glycerol. k_1, k_3, and k_5 represent the rate constants for the forward reactions while k_2, k_4 and k_6 represent the rate constants for the reverse/backward reactions in Eqs. 2–4.

The rate constants and rate determining step were obtained from the established differential equations; Eqs. 6–11 obtained by applying rate law on the sequence of three steps of the reversible decomposition of triglyceride to diglyceride, diglyceride to monoglyceride and monoglyceride to glycerol with a heterogeneous catalyst; calcined banana peel ash catalyst (CBPA) shown in Eqs. 2–4 [24].

Basic assumptions.

1. Concentration of methanol was considered to be excessive compared to concentration of the other reactant constituents

So its concentration is constant hence, the rate equation shown in Eq. 5 obeyed pseudo-first-order kinetics as a function of the concentration of triglyceride. Similarly, other rate expressions Eqs. 6–11 were derived.

2. The catalyst was used in sufficient amount so change in concentration of the catalyst during the course of reaction was assumed to be negligible [25].

The rate equations ensued via relating rate law upon Eqs. 2–4 to determine the rate constants and represented in Eqs. 6–11. The assumptions, rate equations of the different constituents were expressed with constituent mass balances.

$$r_T = {}^{dC_T}/_{dt} = -k_1 T C H_3 OH + k_2 DB \tag{5}$$

Based on the assumptions above, Eq. 5 proceeded by the use of pseudo-first-order-kinetics in relation to the strength of triglyceride T which becomes Eq. 6.

$$r_T = {}^{dC_T}/_{dt} = -k_1 T + k_2 DB \tag{6}$$

The effective rate constant $k_1 = k_1 CH_3 OH$. Other rate equations were derived by using related assumptions of excessive concentration of methanol etc. along these lines;

$$r_D = {}^{dC_D}/_{dt} = k_1 T - k_2 DB - k_3 D + k_4 MB \tag{7}$$

$$r_M = {}^{dC_M}/_{dt} = k_3 D - k_4 MB - k_5 M + k_6 BG \tag{8}$$

$$r_B = {}^{dC_B}/_{dt} = k_1 T - k_2 DB + k_3 D - k_4 MB + k_5 M - k_6 BG \tag{9}$$

$$\mathrm{r}CH_3 OH = {}^{dC_{CH_3OH}}/_{dt} = -k_1 T + k_2 DB - k_3 D + k_4 MB - k_5 M + k_6 BG \tag{10}$$

$$r_G = {}^{dC_G}/_{dt} = k_5 M - k_6 BG \tag{11}$$

The ordinary differential equations (ODE) as shown in Eqs. 6–11 were solved with MATLAB R2014a software to get the rate constants k_1– k_6.

Temperature related terms

Temperature related expressions like activation energy and frequency factor in addition to the reaction order were determined by subjecting the rate constant data of the rate determining step (RDS) of the transesterification reaction to Arrhenius equation given in Eq. 12.

$$\mathrm{K} = k_o \times \exp\left(\frac{-E_a}{RT}\right) \tag{12}$$

$$\ln \mathrm{K} = \left(\frac{-E_a}{RT}\right) + \ln k_o \tag{13}$$

A graph of ln K against $\frac{1}{T}$ was plotted with the experimental data. This gave a straight line slope of $\frac{-E_a}{RT}$ and the frequency factor or pre-exponential factor (k_o) was

calculated from natural log of the intercept (ln k_o) (where T is absolute temperature) for temperatures of 50, 55 and 60 °C and was used to determine E_a and k_o.

Determination of reaction order

Based on the assumption of concentration of methanol continually in excess when compared to the concentration of other reactant species at any given time in the course of the reaction with k as the effective rate constant, order of the reaction n in addition to the effective rate constant k will be found solving Eq. 14.

$$r_T = {}^{dC_T}/_{dt} = -kC_T^n \tag{14}$$

Results and discussion

Lard oil synthesis and oil characterization

The percentage yield of oil derived from lard via dry-rendering method was 96% and has been established to have high oil content. Thus pork lard is suitable for use in oil generation for methyl ester production because of its abundance, oil content, low cost and availability. The use of waste pork fat serve as means of upgrading or converting waste to energy and wealth hence have the capacity to mitigate the cost of feedstock for biodiesel production ensuring an environmentally and economically sustainability route.

Lard oil (LO) physicochemical properties were determined before been used for Lard oil methyl ester (LOME) synthesis and are presented in Table 1. LO was characterized for acid value, free fatty acid, specific gravity, kinematic viscosity, saponification value, iodine value, water content, peroxide value, flash point and refractive index. Lard oil presented slight acid value and free-fatty-acid values of 2.2 mgKOH/gOil and 1.1%. Specific gravity value of LO was determined as 0.915. The kinematic

Table 1 Physicochemical parameters of lard oil (LO)

Properties	Units	Lard oil
Acid value	mgKOH/g oil	2.2
Free fatty acid	%	1.1
Specific gravity (30 °C)	–	0.915
Kinematic viscosity (40 °C)	mm^2/s	80.994
Saponification value	mgKOH/g oil	226.459
Iodine value	gI_2/100 g oil	34.491
Peroxide value	meq/kg	81.40
Water content	%	0.53
Flash point	°C	240
Refractive index (29 °C)	–	1.4625

viscosity was obtained as 80.994 (mm^2/s) which is on the high side. High values of specific gravity and viscosity lead to poor fuel atomization, incomplete combustion and carbon deposition on the injectors when used directly and as such the oil is unsuitable for direct use in a compression ignition engine as a bio-fuel.

Characterization of the ripe banana peel ash catalyst

The uncalcined banana peel ash (UBPA) and the calcined banana peel ash (CBPA) catalysts samples were characterized and interpreted subsequently as summarized below.

Fourier-transform infra-red (FTIR) analysis of the catalysts samples

FTIR spectroscope analysis was carried out on the uncalcined (burnt) and calcined banana peel ash catalyst to detect the functional groups present and the spectrum for each sample is presented in Figs. 1 and 2. The spectra displayed different adsorption peaks or bands in the wavenumber range of 4000–650 cm^{-1}.

In the analysis of the uncalcined banana peel ash (UBPA), the peak at 3280 cm^{-1} is attributed to the O–H bonds bending and stretching vibration due to the presence of water molecules. Conversely, the bands are not detected in the calcined banana peel ash and could be as a result of the thermal treatment at 700 °C. Similar observations were made by Nisar et al. [26], and Balaji et al. [27]. The peaks at 2922 cm^{-1} and 2855 cm^{-1} in UBPA indicate the presence of peaks characteristic of C–H axial deformation in $–CH_2$ and $–CH_3$ groups. The occurrence of peaks at 887 and 895 in UBPA and CBPA is specific to isolated SiO_4 vibration in $CaMgSiO_4$ in relation with Ca^{2+} and Mg^{2+} (Piriou et al. [28]. The peak at 1480 cm^{-1} is ascribed to the asymmetric stretch of CO_3^{2-} group present in the CBPA due to adsorption of atmospheric CO_2 on metal oxides and signifies the presence of Ca, K and other metal carbonates. Similar result

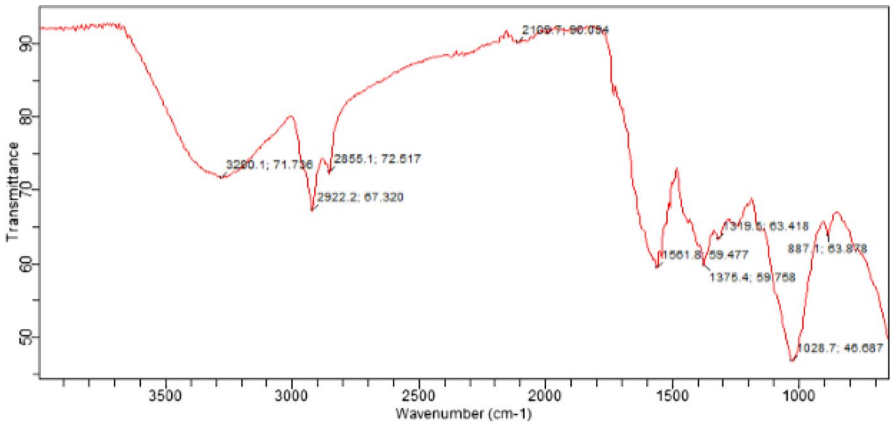

Fig. 1 FT-IR spectra of uncalcined banana peel ash catalyst (UBPA)

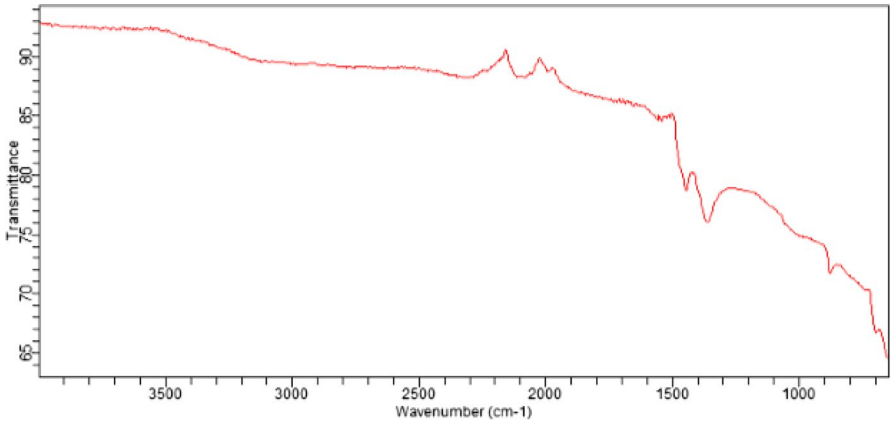

Fig. 2 FT-IR spectra of calcined banana peel ash catalyst(CBPA)

(1474 cm^{-1}) was recorded by Niju et al. [29] in calcined conch shell (CCS). Peaks at 1375 cm^{-1} and 1370 cm^{-1} in UBPA and CBPA are also ascribed to C-O stretching and bending vibration which signifies the presence of carbonate, K_2CO_3 [23, 27]. Furthermore, the peaks at 2350 cm^{-1} and 2120 cm^{-1} in CBPA are assigned to M–O–K bonds (M = Mg, Si, etc.). The variance in the band intensities observed in UBPA and CBPA implies that the calcination temperature (700 °C) significantly extracted the alkali oxide (K_2O), alkaline earth metal oxides (MgO and CaO) and metal oxide (SiO_2). The increased catalytic activity of CBPA could be attributed to the presence of these mixed oxides which was also reaffirmed by the EDAX.

Scanning electron microscopes (SEM) analysis of the ripe banana peel ash catalyst

The surface morphologies of the uncalcined banana peel ash (UBPA) and calcined banana peel ash catalysts (CBPA) executed via SEM taken at magnifications of 500 × and 750 × are depicted in Plates 1(a and b) and Plates 2(c and d). Several aggregates with both mesoporous and microporous structures were observed in the UBPA and CBPA. The UBPA SEM images displayed irregularly deformed coarse surface and voids which could be as a result of the size decrease process conducted in the formulation stage of the catalyst. Surface change of the catalyst was observed from an irregular arrangement in the UBPA to a spongy, fibrous and well-arranged surface microstructure in the CBPA SEM images. This could be attributed to calcination at 700 °C for 4 h. The resulting microstructure suggests the increased surface area of the catalyst which is also relative to the increased catalytic activity of the catalyst after calcination. Similar surface morphology reports were recorded by several authors [17, 23, 27].

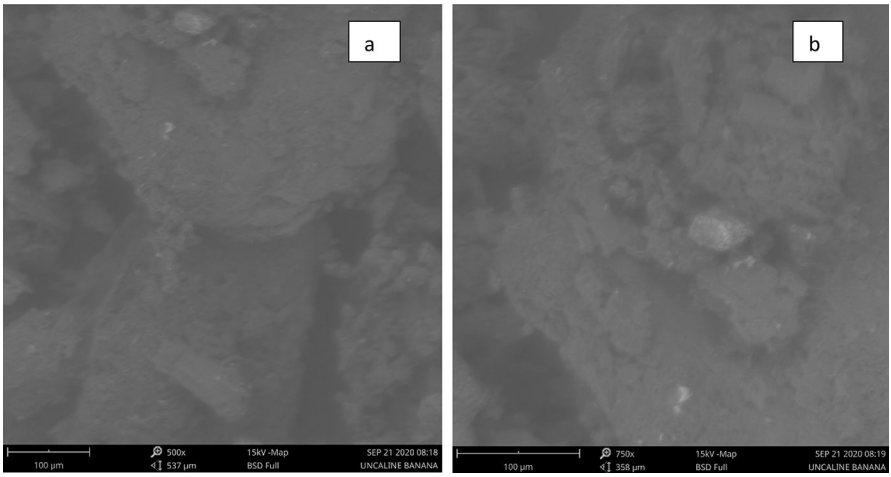

Plate 1 SEM images of uncalcined ripe banana peel ash catalyst (**a** and **b**)

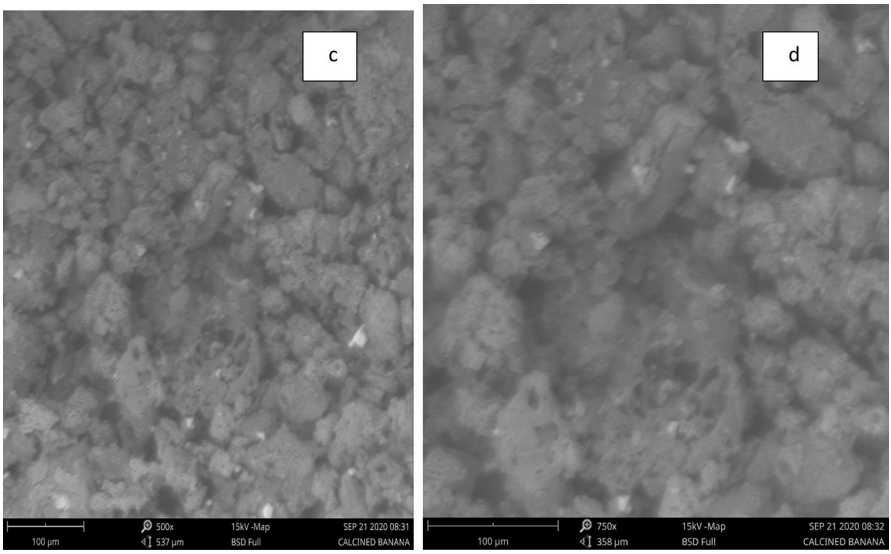

Plate 2 SEM images of calcined ripe banana peel ash catalyst (**c** and **d**)

Energy dispersive atomic X-ray (EDAX) spectroscopy analysis of the ripe banana peel ash catalysts samples

The elemental compositions of the ripe uncalcined banana peel ash UBPA and calcined banana peel ash CBPA were analyzed by EDAX and summarized in Table 2.

The major constituents of the ripe uncalcined and calcined banana peel ash catalysts are potassium (K), chlorine (Cl), calcium (Ca), silver (Ag), niobium

Table 2 Elemental compositions of UBPA and CBPA catalysts obtained using EDAX

Element	Concentration (wt %)	
	UBPA	CBPA
Potassium (K)	46.79	63.71
Oxygen (O)	11.36	8.75
Chlorine (Cl)	6.57	6.31
Calcium (Ca)	6.47	5.26
Carbon (C)	8.00	3.03
Silver (Ag)	5.81	2.26
Niobium (Nb)	1.94	1.73
Phosphorus (P)	1.67	2.35
Silicon (Si)	1.72	1.53
Yttrium (Y)	1.54	1.41
Magnesium (Mg)	1.49	1.38
Aluminium (Al)	3.02	0.65
Sulfur (S)	1.63	0.60
Titanium (Ti)	0.00	0.51
Sodium (Na)	1.31	0.44
Nitrogen (N)	–	0.31
Iron (Fe)	0.00	0.30
Vanadium (V)	–	0.16

(Nb) with potassium reflecting the greatest presence and dominance. Potassium is reported to be a strong base catalyst and is responsible for the strong alkaline character of the catalyst in transesterification reaction. It possesses minor toxicity, high reactivity with water and high basic strength [30]. These results are in accordance with the findings of Mendonca et al. [31], Pathak et al. [18] and Gohain et al. [17]. and also corroborated by the XRD and FTIR analyses.

After calcination, potassium was seen to increase from 46.79 wt% in UBPA to 63.71wt% in CBPA while some of the elements were seen to decrease. The results demonstrated that calcination greatly influenced the elemental composition of the CBPA. Elements such as Nb, Si, Y, Mg, Al, S, Ti, Na, N, Fe and V were found in trace amounts. Birla et al. [32] stated that oxides of these elements that were found in trace amounts are effective substances for transetserification reaction. The alkaline oxides such as CaO, MgO, Na_2O, FeO_3 etc. found in the catalysts will boost the catalysts basic strength whereas the acidic constituents like P_2O_5, SiO_2, SO_3 have the capacity to facilitate esterification of the FFA content in feedstocks [33]. Furthermore, the possession of these mineral oxides from all indications has enriched the catalytic activity of CBPA and inferred increased activity in transesterification reaction.

X-ray diffraction (XRD) analysis of the calcined ripe banana peel ash (CBPA) catalyst

The crystalline compounds present in the ripe CBPA were ascertained via the XRD analysis. Fig. 3 depicts the XRD pattern of the banana peel ash catalyst (CBPA) calcined at 700 °C for 4 h. Several peaks were detected at 2Θ range 2°–70° which is ascribed to the existence of cellulose-hemicellulose-lignin matrix found in most biomass materials that were reduced after calcination [28].

It was observed that the calcined banana peel ash (CBPA) catalyst consists of the following crystalline phases; sylvite (KCl), graphite (C), davyne ($K_2Na_4Ca_2Al_6Si_6O_{24}C_{12}$), chlorocalcite ($KCaCl_3$), periclase (MgO) and quartz (SiO_2). However, the dominant phase was chlorocalcite ($KCaCl_3$) phase. Additionally, potassium (K) was seen to be the major element which existed predominantly in the form of $KCaCl_3$, KCl, $K_2Na_4Ca_2Al_6Si_6O_{24}C_{12}$ and constituted of over 60% of the spotted elements. Additionally, the presence of C, Ca, Cl, O, Na, Al, MgO, SiO_4 were also indicated through XRD. These findings were validated by the FTIR and EDAX analyses.

Brunauer–Emmett–Teller (BET) analysis of the calcined ripe banana peel ash (CBPA) catalyst

Table 3 shows the physicochemical properties of the calcined banana (CBPA), assessed through BET analysis. These properties are the BET surface area (m^2/g), BJH cumulative adsorption pore volume (cc/g) and BJH adsorption pore diameter (nm). The particle size of the catalyst was observed to reduce after calcination which led to an increase in the surface area. This observation suggests that calcination has a great influence on the surface area. Catalytic activity is a function of its specific surface area [30]. This infers that the larger the surface area, the higher the catalytic

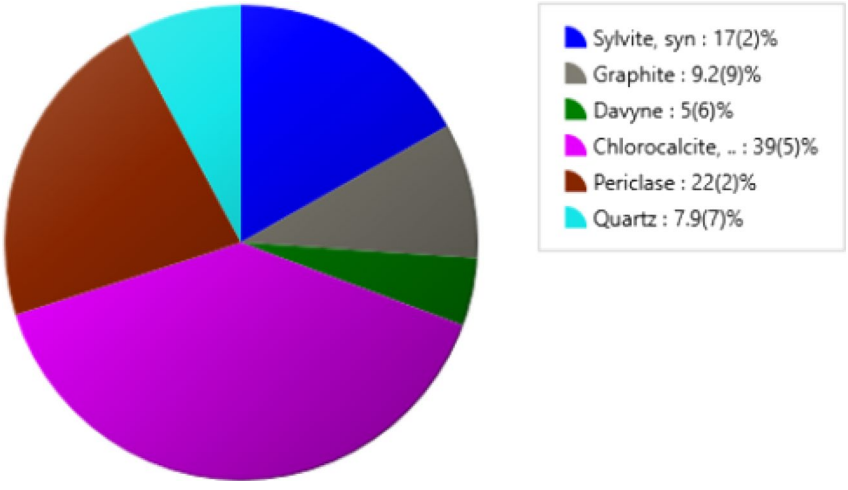

Fig. 3 XRD analysis of calcined banana peel ash (CBPA) catalyst

Table 3 Physicochemical properties of CBPA

Properties	CBPA
BET surface area (m^2/g)	870.8
Pore volume (cc/g)	0.48
Pore diameter (nm)	2.123

activity as catalysts with large surface areas expedites improved interaction between catalyst active sites and reactants.

On comparison between the calcined ripe banana peel ash catalyst CBPA and the uncalcined UBPA as revealed by the characterization results shows higher catalytic activity of CBPA than UBPA thus more suitable to be used for the transesterification reaction of the lard oil.

Lard oil methyl ester fuel properties

Lard oil methyl ester (LOME) produced at optimum process parameters were characterized to determine their physicochemical properties. Table 4 presents succinct fuel properties of lard oil methyl ester LOME with the ASTM limits and EN14214 limits that the fuel properties were measured up to. The LOME properties obtained are within the acceptable limits for fuel and as such suitable to be utilized in internal combustion engine with no further alteration.

Transesterification products distribution

The transesterification of lard oil with methanol heterogeneously catalyzed with CBPA was studied at reaction temperatures of 50 °C, 55 °C and 60 °C. The specified

Table 4 Fuel properties of LOME compared with ASTM limits

Properties	Units	LOME	ASTM limits	EN14214
Acid value	MgKOH/g oil	0.28	0.50 max	0.50 max
Free fatty acid	%	0.14	–	–
Specific gravity (30 °C)	–	0.873	0.86–0.90	0.85
Kinematic viscosity (40 °C)	mm^2/s	4.63	1.9–6.0	3.5–5.0
Saponification value	MgKOH/g oil	199.7	–	
Iodine value	gI_2/100 g oil	32.42	3 min	
Water content	%	–	–	–
Peroxide value	MEq/kg	–	–	–
Cetane number	–	68	47 min	51 min
Higher heating value	MJ/kg	41.1	40–42	
Flash point	°C	135	130 min	120 min
Cloud point	°C	+9	− 3 to 12	–
Pour point	°C	+6	− 15 to 10	–

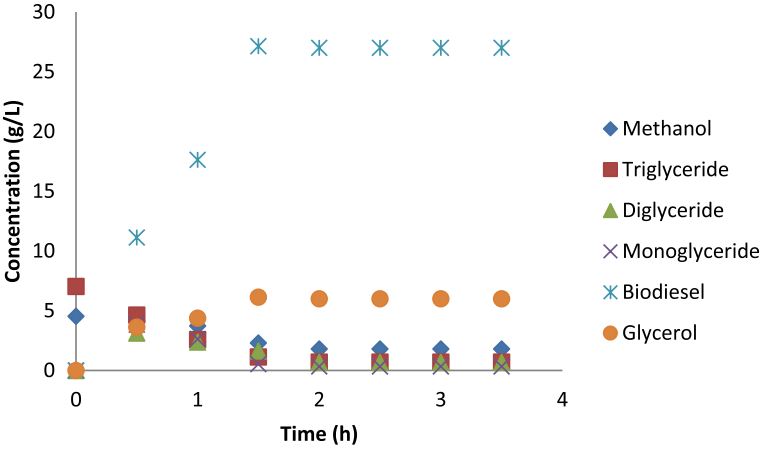

Fig. 4 Concentration of species versus time in lard oil transesterification catalyzed with calcined banana peel ash at 50 °C. Conditions: stir speed of 300 rpm, catalyst amount of 2.5 wt%, methanol:LO proportion of 10.5:1

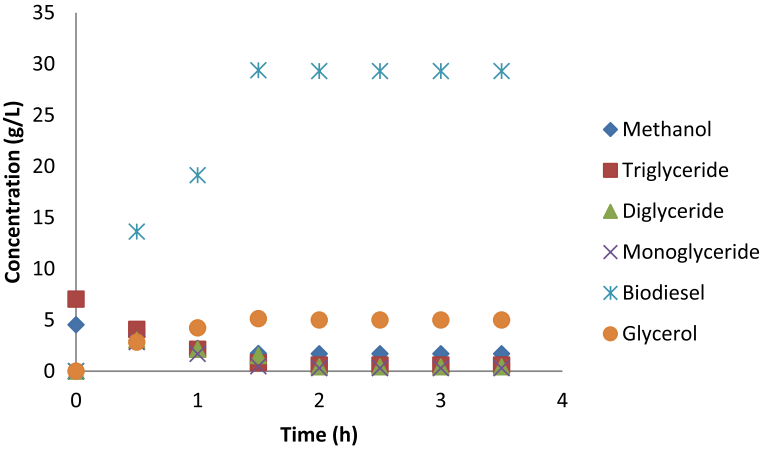

Fig. 5 Concentration of species versus time in lard oil transesterification catalyzed with calcined banana peel ash at 55 °C. Conditions: stir speed of 300 rpm, catalyst amount of 2.5 wt%, methanol:LO proportion of 10.5:1

optimum reaction conditions for the transesterification process are as follows; 10.5:1 methanol/lard oil molar ratio, 2.5 wt% CBPA catalyst concentration (established on lard oil weight). The transesterification reaction followed series of sequential, reversible reactions in stage wise form as indicated in Eqs. 2–4. The dispersal of the transesterification products at the specified optimum conditions and temperatures of 50 °C, 55 °C and 60 °C are depicted in Figs. 4, 5 and 6. Significant variations were seen in the strength of methanol, triglyceride, diglyceride, monoglyceride, lard oil methyl ester and glycerol. The concentration of methanol, triglyceride, diglyceride

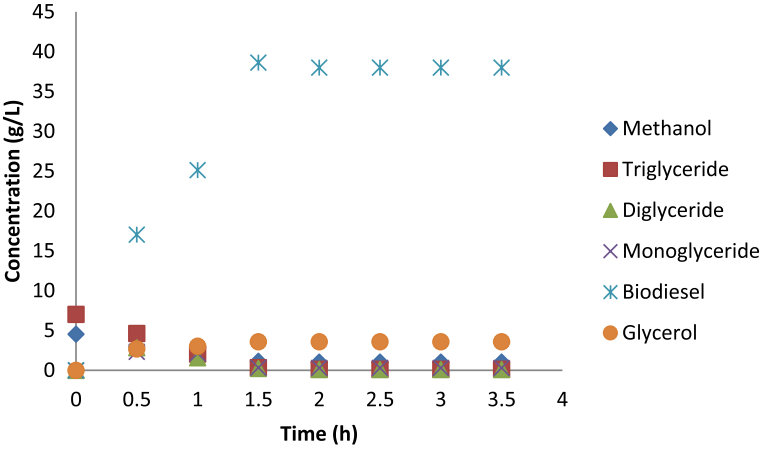

Fig. 6 Concentration of species versus time in lard oil transesterification catalyzed with calcined banana peel ash at 60 °C. Conditions: stir speed of 300 rpm, catalyst amount of 2.5 wt%, methanol:LO proportion of 10.5:1

and monoglyceride were seen to decrease while that of lard oil methyl ester and glycerol increased. A visual inspection of Figs. 4, 5 and 6 shows that the changes in concentration of each of the species (reactants and products) reached its maximum at 1.5 h slightly decreased beyond the time of 1.5 h and remained constant across the temperature readings. This could be as a result of the reaction reaching its end point at 1.5 h. Biodiesel was seen to be prevailing in the product side at a temperature of 60 °C implying that the yield increased with temperature increase from 50 to 60 °C as the reaction proceeded.

Rate determining step (RDS) of LOME synthesis using the reverse basic reaction mechanism (RB)

The developed rate expressions, r CH_3OH, $r_T r_D r_{D,} r_M, r_B, r_G$ in Eqs. 6–11 are based on the six reactions in Eqs. 2–4 which are sequence of reversible breakdowns of tri-glyceride to di-glyceride, di-glyceride to mono-glyceride and mono-glyceride to glycerol. The effectual rate constants (k_1–k_6) distinct in Eqs. 6–11 were computed with the concentration–time data depicted in Figs. 4, 5 and 6 at the defined temperatures of 50 °C, 55 °C and 60 °C. Programs were composed in MATLAB software-version 2014a to decipher the six ordinary-differential- equation ODE given in Eqs. 6–11 with six unknowns. The estimates of the effectual rate constants computed are displayed in Table 5 hence; the rate determining step was established.

The reaction orders for the forward and backward reactions are assumed to be first and second, thus, varying units of k describe the forward and in reverse reactions. The unit of k for the forward reaction is denoted with (h^{-1}) while that of the backward reaction is (L mol^{-1} h^{-1}). Consequently, it is distinct in Table 5 that the rate constant values for the forward reaction (k_1, k_3, k_5) are greater than that of the backward reaction (k_2, k_4, k_6). This entails that the forward reaction dominates and the reverse reactions

Table 5 Rate constants of lard oil transesterification at varying temperatures

Reaction	Rate constant (unit)	Temperature (°C)			ΔE, (kJ/mol)	A (h^{-1})
		50 °C	55 °C	60 °C		
T → D	k_1 (h^{-1})	0.9303	1.0632	1.1702	20.54	1.96×10^3
D → T	k_2 (L mol^{-1} h^{-1})	− 0.0031	− 0.0077	− 0.0206		
D → M	k_3(h^{-1})	1.1938	1.5188	1.6580		
M → D	k_4(L mol^{-1} h^{-1})	0.0116	0.0230	− 0.0078		
M → G	k_5 (h^{-1})	1.1728	1.6813	1.7523		
G → M	k_6(L mol^{-1} h^{-1})	− 0.0049	-0.0076	0.000838		

can be ignored for these experimental settings. The lowest rate constant values for the forward reactions in dominance are that obtained from the conversion of tri-glyceride to di-glyceride across all the temperature readings (50 °C, 55 °C and 60 °C) thus regarded as the rate determining step (RDS). This is in agreement with the findings of Mu'azu et al. [34]. The kinetic parameters of the reverse reaction of di-glyceride to tri-glyceride were all negative values and they were also rejected based on the recorded negative values. This corroborates the report of Mucino et al. [35] which stated that models are rejected based on distinct trend from the experimental data or kinetic parameters with erroneous values such as negative values, too high values or not significantly different from zero at the 95% confidence level. Table 5 shows that the effectual rate constants of the rate determining step raised from 0.9303 to 1.0632 then to 1.1702 h^{-1} as the temperature rose from 50 °C to 55 °C and to 60 °C. As the rate determining step of lard oil transesterification is favored at higher temperatures, whereby the optimum concentration of methyl ester was obtained at 60 °C (Fig. 6) it signifies that the reaction is an endothermic reaction.

Modeling and simulation of lard oil transesterification catalyzed with CBPA

The rate constants calculated at the different temperatures, 50 °C, 55 °C, 60 °C were later substituted in the rate determining step (T → D) equation to estimate the rate of reaction in relations to conversion of tri-glyceride in LOME synthesis. It was followed by simulation with Matlab software (version 2014a) and the graphical representation illustrated in Figs. 7, 8 and 9. A satisfactory relationship was seen to be amid the experimental and predicted values in the Figures. This was also evidenced by the high coefficient of determination (R^2) recorded at the varying temperatures 50 °C, 55 °C, 60 °C shown in Table 6. This infers the accuracy of the predicted rate constants.

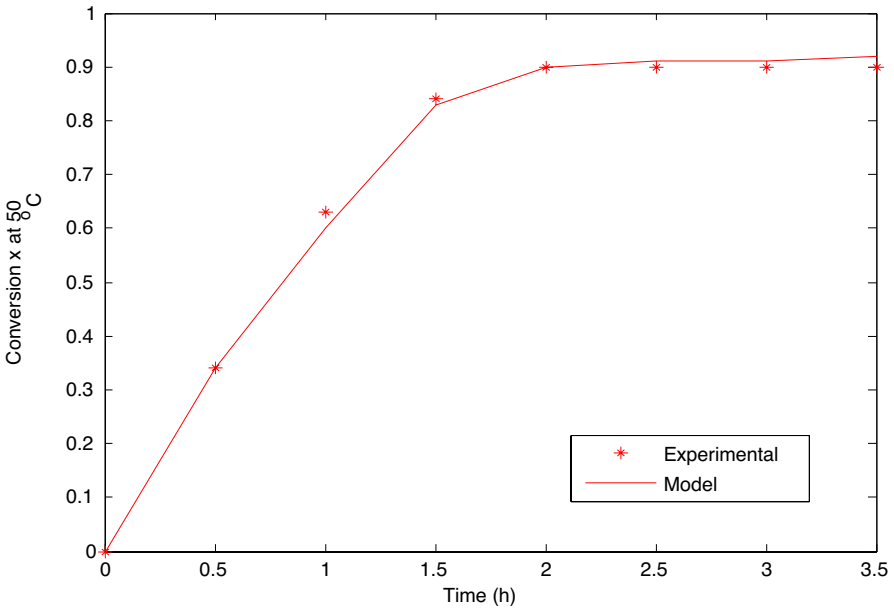

Fig. 7 Extrapolation of lard triglyceride conversion versus time for RB model at 50 °C. Conditions: stir speed of 300 rpm, catalyst amount of 2.5 wt%, methanol:LO proportion of 10.5:1

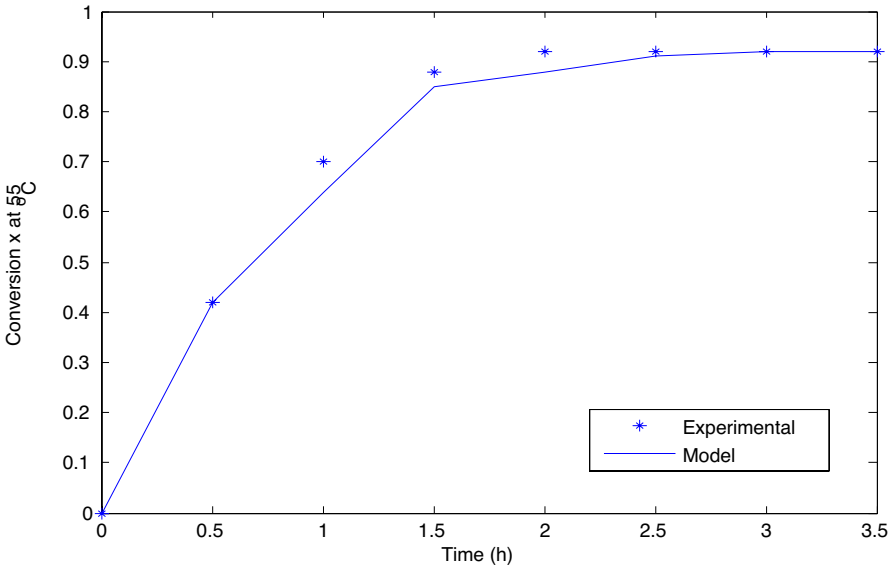

Fig. 8 Extrapolation of lard triglyceride conversion versus time for RB model at 55 °C. Conditions: stir speed of 300 rpm, catalyst amount of 2.5 wt%, methanol:LO proportion of 10.5:1

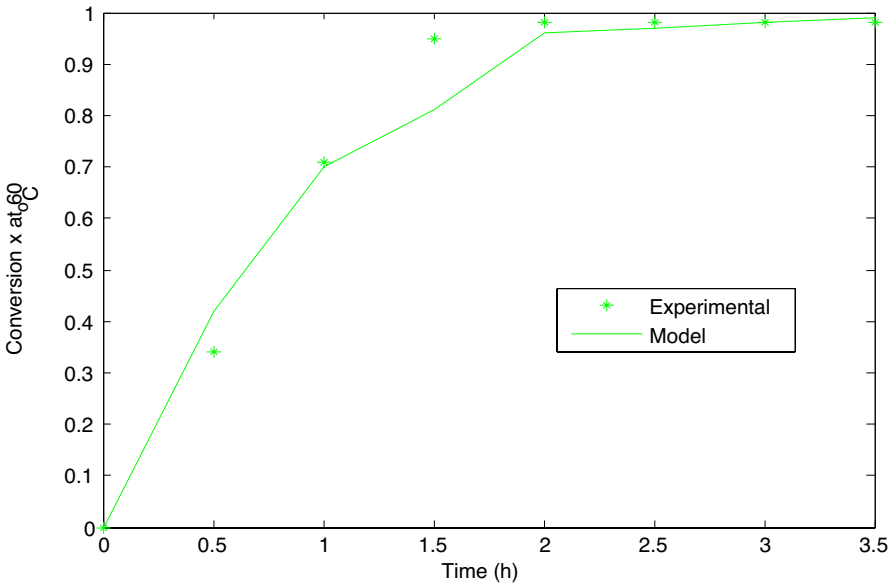

Fig. 9 Extrapolation of lard triglyceride conversion versus time for RB model at 60 °C. Conditions: stir speed of 300 rpm, catalyst amount of 2.5 wt%, methanol:LO proportion of 10.5:1

Table 6 Statistical parameters of the RDS for the reverse basic (RB) model

Reaction mechanism	Temperature (°C)	Coefficient of determination (R^2)
RB	50 °C	0.9982
	55 °C	0.9982
	60 °C	0.9955

Arrhenius parameters of the rate determining step (RDS) of LOME using the reverse basic reaction mechanism (RB)

Activation energy (Ea) is the minimum energy required for a reaction to occur. Catalysts function by decreasing the activation energy in a reaction. It should be noted that the lower the activation energy, the easier it is for a reaction to take place. A graph of ln k against $\frac{1}{T}$ was plotted (Fig. 7) using the experimental data for k_1 on Table 5 (where T is absolute temperature) for temperatures of 50, 55 and 60 °C and was used to determine E_a and A.

The estimates of the activation energy as well as the frequency factor as calculated from Fig. 10 are 20,535.58 J/mol or 20.54 kJ/mol and 1.96×10^3 h^{-1}. This implies that the minimum energy required for the conversion of lard oil to LOME with CBPA catalyst is 20.54 kJ and the pre-exponential factor A is 1.96×10^3 h^{-1}.

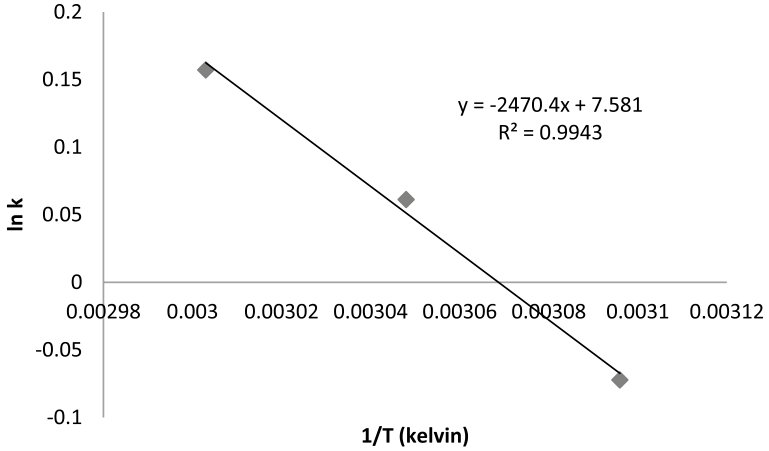

Fig. 10 Arrhenius plot of ln k versus 1/T for k_1 of LOME rate determining step in reverse basic mechanism

This shows that the reaction is mass transfer resistant and endothermic. Low activation energy is preferred because it is the least energy requisite to induce a chemical reaction.

It is worthy to note that activation energy is subjected to the reaction fusion (quality of oil, alcohol and catalyst) as well as the reaction preconditions [36].

Development of kinetic rate equation of the rate determining step (RDS) of LOME using the reverse basic reaction mechanism (RB)

The concentration–time data of the rate determining step (RDS) at 60 °C shows the LO transesterification reaction is first order (n = 1). This implies conversion of tri-glyceride to lard oil methyl ester in the existence of excess methanol ensues via first order kinetics. The values of Ea, k_o, R and n are substituted in Eq. 14; $r_T = {}^{dC_T}/_{dt} = -kC_T^n$ and Eq. 12; $k = k_o e^{-Ea/RT}$. Using the rate determining step (Tri-glyceride conversion to Di-glyceride) based on the reverse basic reaction mechanism, the rate equation for lard oil transesterification reaction with calcined banana ash catalyst (CBPA) as heterogeneous catalyst is given by Eq. 15.

$$\begin{aligned} r_T = {}^{dC_T}/_{dt} &= k_o e^{-Ea/RT} C_T\left(1-X_T\right); \text{But } C_T = C_{To}\left(1-X_T\right) \\ {}^{dC_T}/_{dt} &= k_o \times C_{To} \times \exp^{(-Ea/RT)} \times \left(1-X_T\right) \\ &= 1960.6 \times C_{To} \times \exp^{(-20536)/8.314\times T)} \times C_T\left(1-X_T\right) \end{aligned} \quad (15)$$

Conclusion

In this study, calcined banana peel ash catalyst was used as a heterogeneous catalyst in the catalysis of the methanolysis of lard oil in lard oil methyl ester synthesis. The kinetic analysis disclosed the data fitted reverse basic (RB) kinetic model proposed by Freedman with triglyceride conversion to diglyceride as the rate determining step. Thus a new kinetic model which describes the kinetics of lard oil transesterification using calcined banana peel ash as heterogeneous catalyst was developed as shown in Eq. 15. The reaction been favored as the temperature increased confirms the endothermic nature of the lard oil transesterification reaction which suggests an increase in the rate of diffusion between the three-interphase (oil-methanol-catalyst) because of the increase in temperature. The activation energy and frequency factor of 20.54 kJ/mol and 1.960 h^{-1} obtained implies that the catalyst effectively lowered the energy barrier of the transesterification reaction and as such should be sought after to be used for an economical and sustainable methyl ester synthesis.

Acknowledgements The authors did not receive any funding from any organization for conducting this study.

Author contributions Conceptualization, methodology, formal analysis and investigation, writing—original draft preparation: [ECB]; Writing—review and editing: [UCF]; Supervision: OOD: Proof reading: [ECN].

Data availability Not applicable.

Declarations

Competing interest The authors have no competing interests to declare that are relevant to the content of this article.

References

1. Anwar M, Rasul MG, Ashwath N, Nabi-Nurun MD (2019) The potential of utilizing papaya seed oil and stone fruit kernel oil as non-edible feedstock for biodiesel production in Australia—a review. Energy Rep 5:280–297
2. Martini N, Schele JS (2012) Plant oils as fuels: present state of science and future developments. Springer, Berlin
3. Singh D, Sharma D, Soni SL, Sharma S, Kumar Sharma P, Jhalani A (2020) A review on feedstocks, production processes, and yield for different generations of biodiesel. Fuel 262:116553
4. Folayan AJ, Anawe PAL, Aladejare AE, Ayeni AO (2019) Experimental investigation of the effect of fatty acids configuration, chain length, branching and degree of unsaturation on biodiesel fuel properties obtained from lauric oils, high oleic and high- linoleic vegetable oil biomass. Energy Rep 5:793–806
5. Leung DYC, Wu X, Leung MKH (2010) A review on biodiesel production using catalyzedtransesterification. Appl Energy 87:1083–1095
6. Konwar LJ, Das R, Thakur AJ, Salminen E, Maki-Arvela P, Kumar N, Mikkola JP, Deka D (2014) Biodiesel production from acid oils using sulfonated carbon catalyst derived from oilcake waste. J Mol Catal A: Chem 388:167–176

7. Ude CN, Onukwuli OD (2019) Kinetic modeling of transesterification of gmelina seed oil catalyzed by alkaline activated clay (NaOH/clay) catalyst. React Kinet Mech Catal 127:1039–1058
8. Demirbas A, Bafail A, Ahmad W, Sheikh M (2016) Biodiesel production from non-edible plant oils. Energy Explor Exploit 34(2):290–318
9. Al-dobaini IA, Fadhil AB, Saeed IK (2016) Optimized alkali-catalyzed transesterification of wild mustard (*Brassica juncea* L.) seed oil. Energy Sources Part A 38(15):2319–2325
10. Ezekannagha CB, Ude CN, Onukwuli OD (2017) Optimization of the methanolysis of lard oil in the production of biodiesel with response surface methodology. Egypt J Pet 26(4):1001–1011
11. Aliozo OS, Emembolu LN, Onukwuli OD (2017) Optimization of melon oil methyl ester production using response surface methodology. Biofuels Eng 2(1):1–10
12. Onukwuli OD, Esonye C, Ofoefule AU, Eyisi R (2021) Comparative analysis of the application of artificial neural network genetic algorithm and response surface methods- desirability function for predicting the optimal conditions for biodiesel synthesis from chrysophyllum albidum seed oil. J Taiwan Inst Chem Eng. https://doi.org/10.1016/j.jtice.2021.06.012
13. Oke EO, Adeyi O, Okolo BI, Ude CJ, Adeyi JA, Salam KK, Nwokie U, Nzeribe I (2021) Heterogeneously catalyzed biodiesel production from Azadiricha Indica oil: predictive modeling with uncertainty quantification, experimental optimization and techno-economic analysis. Biores Technol 332:125141
14. Ezekannagha CB, Nwabueze HO, Ekete JA (2016) Empirical models and rheology of some basic properties of lard biodiesel and their blends with diesel fuel. J Emerg Trends Eng Appl Sci Scholarlink Res 7(3):149–160
15. Hussain F, Alshahrani S, Abbas MM, Khan HM, Jamil A, Yaqoob H, Soudagar MEM, Imran M, Ahmad M, Munir M (2021) Waste animal bones as catalysts for biodiesel production; a mini review. Catalysts 11:630
16. Kumar M, Sharma MP (2016) Selection of potential oils for biodiesel production. Renew Sustain Energy Rev 56:1129–1138
17. Gohain M, Devi A, Deka D (2017) Musa balbisiana colla peel as highly effective renewable heterogeneous base catalyst for biodiesel production. Ind Crops Prod 109:8–18
18. Pathak G, Das D, Rajkumari K, Rokhum (2018) Exploiting waste: towards a sustainable production of biodiesel using Musa acuminate peel ash as a heterogeneous catalyst. Green Chem 20(10):2365–2373
19. Mucino GE, Romero R, Ramirez A, Ramos MJ, Beeza-Jimenez R, Natividad R (2016) Kinetics of transesterification of safflower oil to obtain biodiesel using heterogeneous catalysis. Int J Chem React Eng 14(4):1–10
20. Levenspiel O (2000) Chemical reaction engineering. John Wiley and Sons Inc, Delhi, pp 11–75
21. Onukwuli OD, Ude CN (2018) Kinetics of African pear seed oil (APO) methanolysis catalyzed by phosphoric acid-activated kaolin clay. Appl Petrochem Res 8:299–313
22. Alptekin E, Canakci M (2011) Determination of the density and the viscosities of biodiesel-fuel blends. Renew Energy 33(12):2623–2630
23. Betiku E, Akintunde AM, Ojumu TV (2016) Banana peels as a biobase catalyst for fatty acid methyl esters production using napoleon's plume (*Bauhinia monandra*) seed oil: a process parameters optimization study. Energy 103:797–806
24. Freedman B, Butterfield R, Pryde EH (1986) Transesterification kinetics of soy bean oil. J Am Oil Chem Soc 63(10):1375–1380
25. Zhang L, Sheng B, Xin Z, Liu Q, Sun S (2010) Kinetics of transesterification of palm oil and dimethyl carbonate for biodiesel production at the catalysis of heterogeneous base catalyst. Biores Technol 101:8144–8150
26. Nisar J, Razaq R, Farooq M, Igbal M, Khan RA, Sayed M, Shah A, Ur Rahman I (2017) Enhanced biodiesel production from jatropha oil using calcined waste animal bones as catalyst. Renew Energy 101:111–119
27. Balajii M, Niju S (2020) Banana peduncle—a green and renewable heterogeneous base catalyst for biodiesel production from *Ceiba pentandra* oil. Renew Energy 146:2255–2269
28. Piriou B, Mcmillan P (1983) The high-frequency vibrational spectra of vitreous and crystalline orthosilicates. Am Miner 68(3–4):426–443
29. Niju S, Anushya C, Balajii M (2019) Process optimization for biodiesel production from *Moringa oleifera* oil using conch shells as heterogeneous catalyst. Environ Prog Sustain Energy 38(3):e13015

30. Tshizanga N, Aransiola EF, Oyekola O (2017) Optimisation of biodiesel production from waste vegetable oil and eggshell ash. S Afr J Chem Eng 23:145–156
31. Mendonca IM, Paes OAR, Maia PJS, Souza MP, Almeida RA, Silva CC, Duvoisin S, De Freitas FA (2019) New heterogeneous catalyst or biodiesel production from waste tucuma peels (*Astrocarum aculeatum* Meyer): parameters optimization study. Renew Energy 130:103–110
32. Birla A, Singh B, Upadhyay SN, Sharma YC (2012) Kinetics studies of synthesis of biodiesel from waste frying oil using a heterogeneous catalyst derived from snail shell. Biores Technol 106:95–100
33. Boey PL, Maniam GP, Hamid SA (2011) Performance of calcium oxide as a heterogeneous catalyst in biodiesel production: a review. Chem Eng J 168:15–22
34. Muazu K, Mohammed-Dabo IA, Waziri SM, Ahmed AS, Bugaje IM, Zanna UAS (2015) Kinetic modeling of transesterification of *Jatropha curcas* seed oil using heterogeneous catalyst. Eng Technol 2(3):87–94
35. Mucino GE., Romero R., Ramirez A, Ramos MJ, Beeza-Jimenez R, Natividad R (2016) Kinetics of transesterification of safflower oil to obtain biodiesel using heterogeneous catalysis. International Journal of Chemical Reaction Engineering, 14 (4):1 – 10.
36. Gude VG, Martinez-Guerra E (2018) Green chemistry with process intensification for sustainable biodiesel production. Environ Chem Lett 16(2):327–341